# PROBING LUMINESCENCE IN THE COLLISIONS OF FURAN MOLECULES WITH DIHYDROGEN CATIONS USING COLLISION-INDUCED EMISSION SPECTROSCOPY

TOMASZ J. WASOWICZ

Division of Complex Systems Spectroscopy, Institute of Physics and Applied Computer Science, Faculty of Applied Physics and Mathematics, Gdansk University of Technology, ul. G. Narutowicza 11/12, 80-233 Gdańsk, Poland
*E-mail:* tomasz.wasowicz1@pg.edu.pl

*Received August 12, 2024*

*Abstract*. Optical spectroscopic studies of furan molecules ($C_4H_4O$) impinged by dihydrogen cations ($H_2^+$) were for the first time performed employing collision-induced emission spectroscopy at ions incident energy range of 25–1000 eV corresponding to the velocities from 49 to 311 km/s. The recorded spectra reveal strong luminescence of atomic hydrogen Balmer lines whose intensities weaken with rising principal quantum number *n*. The spectra also display emission bands of CH radicals excited to the first $A^2\Delta$ and second $B^2\Sigma^-$ electronic states. The emission yield curves of these excited products were additionally measured by recording resultant intensities at different projectile energies. Impact processes are unveiled based on these results.

*Key words*: Furan, cancer, collisions, dissociation, luminescence.

DOI: https://doi.org/10.59277/RomJPhys.2024.69.204

## 1. INTRODUCTION

Ion-molecule interactions are inherent to many natural phenomena. For instance, they are fundamental processes in the generation and evolution of many gas-phase species in the interstellar medium and the atmospheres of planets [1, 2]. Ion-molecule collisions also outline various aspects of manufactured reactions exploited in engineering. For example, knowledge of the basic features of the etching and deposition processes induced by focused ion beams allows the development of efficient techniques for processing and fabrication [3]. However, the most significant necessity for detailed data on ion-molecule collisional processes is observed in medicine. This requirement stems from the possibility of using ions in hadron therapy [4, 5], which appears to be one of the most effective ways of destroying malignant cells by irradiating deep-seated tumors. Cells are damaged by splitting the bonds in their building blocks by primary ionizing beams and secondary particles produced in the surrounding media along the central beam path [4, 6]. Therefore, experimental studies on the fragmentation processes of RNA

and DNA helix backbone molecules, such as deoxyribose sugar, nitrogen bases, and their analogs, triggered by ion impact are highly required.

One such biological compound is furan. A five-membered heterocyclic aromatic ring of furan ($C_4H_4O$) provides a structural entity of many organic and biologically active molecules. It is, for example, a building unit of vitamin B12 and biotin [7] or occurs in the products of the pyrolysis of coals [8]. More importantly, furan is often considered an elementary gas phase analog of deoxyribose [9]. Regarding this context, its neutral dissociation triggered by ions was investigated in a few works [10–13]. These studies concentrated on unraveling the processes preceding the fragmentation of the furan molecules, mainly under the impact of the atomic cations. The isomerization, electron capture, dissociative ionization, dissociative excitation, and complex formation mechanisms were identified by combining the measured results with the *ab initio* calculations [10–13].

This paper presents the first-time measurement of the optical spectra resulting from collisions between furan and dihydrogen molecules. Analysis of these spectra made it possible to suggest another collisional process preceding furan fragmentation. We find a direct dissociative excitation of $H_2^+$ projectiles. Indeed, $H_2^+$ is a molecule, and similarly to furan, it can decompose during collisions. Other impact processes and molecular fragmentation pathways are also discussed.

## 2. EXPERIMENT

The experiments were carried out at the University of Gdansk using collision-induced emission spectroscopy (CIES) as described in detail in [13–15]. The state-of-the-art spectrometer and the measurement method are discussed in [13, 14]. Therefore, only an outline and data relevant to furan are provided here.

The spectrometer comprises dedicated vacuum chambers for the cation source, the magnetic mass selector, the collision cell, and the optical detection system. The first stage contained the Colutron ion source with a cathode that generated dihydrogen cations from the $H_2$ gas at 50 and 100 Pa pressures. The cations in the plasma were pulled by an electric potential of 1000 V and guided to a 60° magnetic mass selector. The beam was filtered to cations of the specified $m/z$ ratio in this mass selector. They were then slowed to the required velocity/energy by electrostatic lenses and injected into the collision cube. In the collision area, the cations penetrated the furan vapors. This interaction divided the furan into fragments. The luminescence of the emitting fragments was captured using an optical assembly equipped with a McPherson 218 spectrograph crossed with a 1024-channel "Mepsicron" multichannel photon detector.

High-resolution spectra $\Delta\lambda$ of 0.4 nm (FWHM) at constant ion energy were first measured using a 1200 l/mm grating to identify the products of this

interaction. The luminescence of the identified spectral line or molecular band was scanned over the studied energy range using a 300 l/mm grating, which has a lower resolution but transmits higher intensity. This measurement was carried out in the 25–1000 eV energy range of the $H_2^+$ cations corresponding to the velocities from 49 to 311 km/s. The ion beam currents were controlled simultaneously with the photon emission counts to scale the photon signals properly. The $H_2^+$ beam current in the collision region was about 0.2 nA at 25 eV, increasing to 34 nA at 850 eV and decreasing towards 10 nA at 1000 eV. The signal was acquired several times at every energy to realize good statistics. Each such spectrum then had a correction for the wavelength dependence of the sensitivity of the optical device. The intensity of an individual emission line or band was obtained by integrating over its area and normalizing to accumulating time, $H_2^+$ current, and furan pressure. This procedure gives relative emission cross-sections (σ) for forming these emitting products.

Furan was procured from Sigma Aldrich. The supplier reported a purity of 99%. Although furan is a liquid, it is highly volatile (605.2 mmHg at 25°C [16]). It was, therefore, introduced into the gas line without heating. Instead, it was degassed by several freeze-pump-thaw cycles. The pressure of the furan was set at 15 mTorr and monitored by the Barocel capacitance manometer.

## 3. RESULTS AND DISCUSSION

The high-resolution optical fragmentation spectrum of furan measured for collisions with the $H_2^+$ cations is shown in Fig. 1. We can distinguish the spectral lines of the Balmer series, $H_\beta$ to $H_\varepsilon$, due to the excitation of atomic hydrogen to the H($n$) states, $n$ = 4–7, and bands of the vibrationally and rotationally excited CH radical occurring *via* $A^2\Delta \rightarrow X^2\Pi_r$ and $B^2\Sigma^+ \rightarrow X^2\Pi_r$ electronic transitions.

For over a decade, we have explored the effects of charged particles [10–15], [17–25] and photons [26–32] on five- and six-membered heterocyclic molecules. We, therefore, have a substantial amount of experimental data to compare with the present results.

Specifically, the present spectrum bears a resemblance to the spectrum obtained in the $H^+$+furan [13] collisions. We observed a similar resemblance in the collisions of tetrahydrofuran (a hydrogenated analog of furan) with protons [13, 14] and dihydrogen cations [21]. Both cations did not lead to efficient dissociation of the target molecules. All the data suggest that the charge transfer process dominates collisions with $H^+$ and $H_2^+$. Indeed, the much heavier cations induced significant decompositions of all the molecules hitherto studied. This led to the formation of many fragments that luminesced intensely [14, 15, 19, 20, 22].

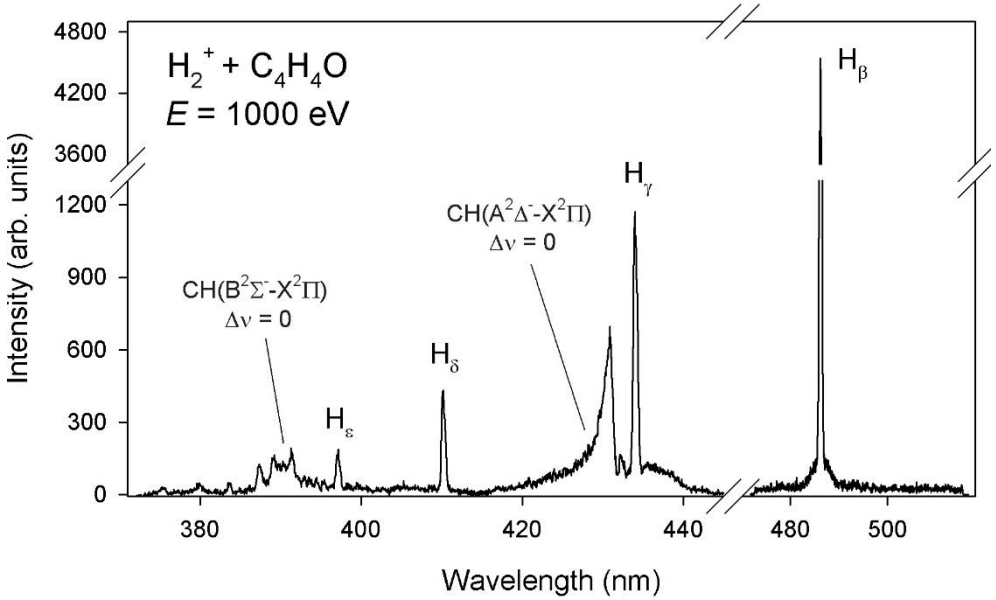


Fig. 1 – Collision-induced luminescence spectrum measured at 1000 eV with an optical resolution Δλ of 0.4 nm for collisions of the furan molecules with $H_2^+$ cations. The major features are assigned. The spectrum was not corrected for the wavelength dependence of the sensitivity of the detection system.

This was because charge transfer reaction no longer played an important role, and other processes (for more details, see, *e.g.* [22]) led to dissociation. This situation is similar to photon irradiation [26–32], where the charge transfer reaction does not occur.

Figures 2a and 2b show emission yields of all excited fragments that were obtained in collisions of $H_2^+$ cations with furan. Experimental uncertainties of the emission yields are standard deviations from several independent measurements performed at each impact energy. The energy scale uncertainty is not shown here because it was estimated to be less than 3.5%, considering the target's ion beam energy spread and thermal motion.

All the curves obtained in collisions of dihydrogen cations with furan increase with velocity and reach the first maximum at around 180 km/s (350 eV). They again rise above ~280 km/s (850 eV), but this time very rapidly to a maximum of 310 km/s (1000 eV).

Figures 2a and 2b also show the emission yield curves for the H($n$ = 4) and $CH(A^2\Delta)$ fragments obtained in collisions between furan and protons [13]. In the velocity range studied here, both these curves are very similar to yields obtained here for $H_2^+$ + furan collisions. This suggests a similarity in the processes that took place in both collisional systems.

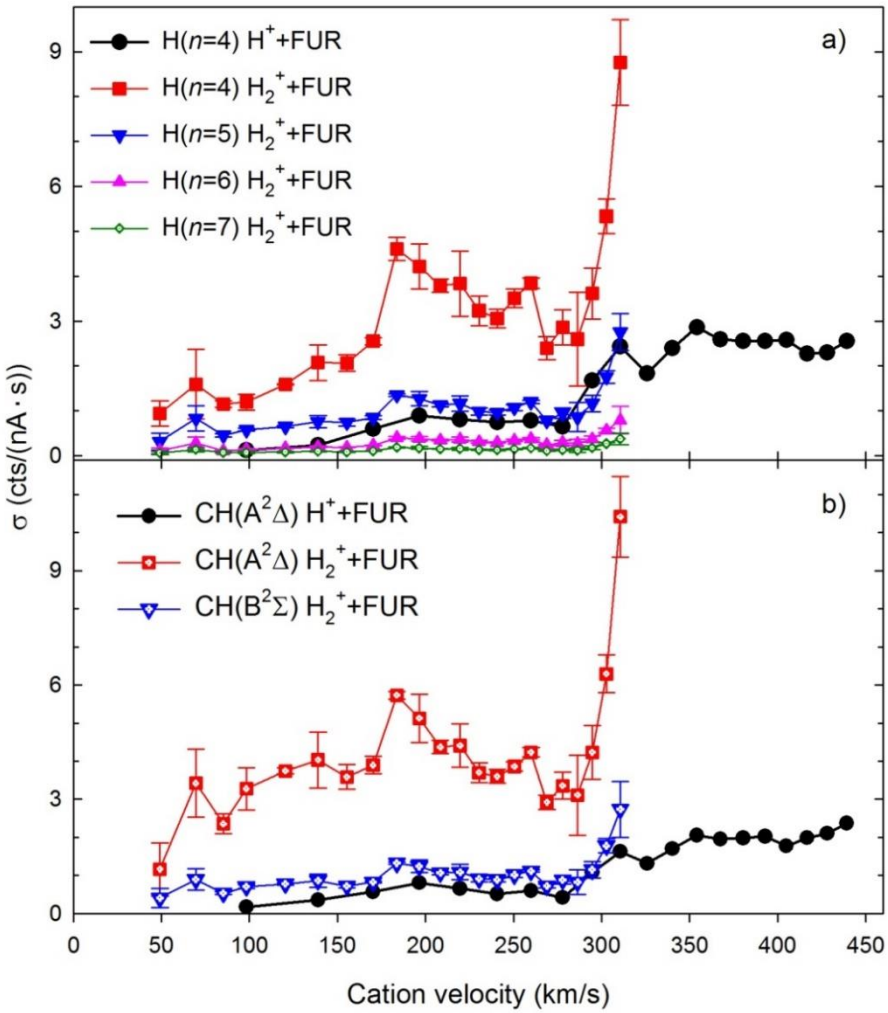


Fig. 2 – Emission yields of the excited fragments obtained in collisions of $H_2^+$ cations with furan.

Average relative abundances (*RA*) of luminescence products were calculated to determine trends in different impact systems involving protons and dihydrogen projectiles. *RA* is defined as the fractional yields of individual excited fragments to the total yield of all identified emitting products (recorded at 190–520 nm wavelength) and averaged over the whole cation energy range (25–1000 eV). *RA* given in this form represents an approximate trend, as it does not include $H_\alpha$, which emission was outside the sensitivity range of our detector. Table 2 shows the *RA* results from $H^+$ and $H_2^+$ impact on the furan molecule. The *RA* values derived from $H^+$ and $H_2^+$ collisions with tetrahydrofuran [13, 21], and pyridine [22] are also presented in Table 1 for comparison.

*Table 1*

Average relative abundances of emitting fragments, *RA* (in %). The results of collisions of protons and dihydrogen cations with tetrahydrofuran [13, 21], as well as pyridine [22], are shown for comparison

| | Furan ($C_4H_4O$) | | Tetrahydrofuran ($C_4H_8O$) | | Pyridine ($C_5H_5N$) | |
|---|---|---|---|---|---|---|
| Emitter | $H^+$ | $H_2^+$ | $H^+$ | $H_2^+$ | $H^+$ | $H_2^+$ |
| H($n$ = 4–7) | 58.3 | 46.3 | 88.8 | 76.2 | 61.4 | 45.9 |
| CH(A,B,C) | 39.9 | 51.0 | 11.2 | 23.8 | 26.9 | 40.4 |
| Other | 1.9 | 2.7 | – | – | 11.7 | 13.7 |

In all these impact systems, the production of excited hydrogen atoms decreases with increased hydrogen cation mass. The *RA* of hydrogens obtained for furan and pyridine are at similar levels. Also, the *RA* summed for the other fragments is at a similar range for both molecules, although CH production from the dissociation of pyridine was lower. It can, therefore, be concluded that the effect of protons on these molecules is almost the same. Similarly, the influence of $H_2^+$ will produce a similar result regardless of the target. Our previous analyses [13–15, 21, 22] suggested that protons and $H_2^+$ mainly interact with molecular targets *via* electron transfer reactions, which somehow limits further fragmentation pathways. Indeed, electron transfer is an exothermic process in all the reactions compared here (see Table 2). It is, therefore, the most energy-efficient process. The channels leading to the formation of excited hydrogens are enhanced because these products may come from both the projectiles and targets. In principle, it should be assumed that the excited hydrogen fragments are more likely to come from projectiles. In earlier works [13, 14], we have shown that there is a parameter whose value can indicate the source of the hydrogen fragments. This parameter is the depopulation factor of the higher-lying electronic states of hydrogen.

*Table 2*

Thermochemical estimation of the lowest threshold energies ($E_{TH}$) for electron transfer reactions. The energies used in the calculations were taken from the NIST Database [33]

| Reactants | Products | $E_{TH}$ [eV] |
|---|---|---|
| $H^+$+$C_4H_4O$ | H+$C_4H_4O^+$ | –4.72 |
| $H_2^+$+$C_4H_4O$ | $H_2$+$C_4H_4O^+$ | –6.55 |
| $H^+$+$C_4H_8O$ | H+$C_4H_8O^+$ | –4.20 |
| $H_2^+$+$C_4H_8O$ | $H_2$+$C_4H_8O^+$ | –6.03 |
| $H^+$+$C_5H_5N$ | H+$C_5H_5N^+$ | –4.34 |
| $H_2^+$+$C_5H_5N$ | $H_2$+$C_5H_5N^+$ | –6.17 |

Under normal excitation of the hydrogen atomic fragments in their consecutive ($n$, $l$) substates populated according to their statistical weights ($2l$+1), the intensities of

the successive Balmer lines should decrease according to the $n^{-3}$ dependency [34]. H($n$) intensities have been found to follow the $n^{-3}$ relation in recent studies of electron- [17] and photon-induced [32, 35] dissociation of similar five-membered heterocyclic molecules. Furthermore, the H($n$) intensities of hydrogen atoms from $C^+/O^+$+THF collisions have obeyed this rule [14]. However, if the hydrogen cations move with significant velocities in a magnetic field (this is the case with hydrogen cation projectiles), an electric field can be induced, altering the branching ratios and lifetimes of individual states. Higher velocities produce larger electric fields, which have a more significant effect. At this point, the reader is referred to the articles of Windholz and co-workers [36, 37], in which the influence of an electric field on electronic states is shown, namely the occurrence of transitions strictly forbidden without field and the generation of level-anticrossing effects resulting from mixing between states of different principal quantum numbers and between singlet and triplet states of helium. Therefore, the mixing of states and suppressing populations may also occur for hydrogen cations [34], rapidly decreasing the Balmer lines' intensities. This is reflected in the lower value of the depopulation factor, which is no longer –3. In fact, depopulation factors are lower than –3 in the entire velocity range. In particular, our analysis shows that at lower velocities, depopulation values rapidly decrease from −4.2 to –5.7, and above 200 km/s, they linearly rise to –5.2. Very similar trends were observed for $H^+/H_2^+$ collisions with THF [13, 14, 21] and pyridine [22]. However, the average value of the depopulation factor for $H_2^+$ cations is usually 0.6 higher than that of protons. It seems that this observation may originate in the fragmentation of the hydrogen molecule after the projectile has been neutralized in the charge transfer reaction. This reaction may slightly slow down the movement of the hydrogen molecule and, later, the newly formed hydrogen fragment. Interestingly, in the $H_2^+$ + $ND_3$ collisions [38], dissociative excitation of the $ND_3$ target molecule was mainly observed instead of a charge transfer reaction. Indeed, the cross-section measured at 1000 eV for the production of excited ND radical was determined to be 50 times higher than the cross-section for the production of hydrogen atoms.

## 4. SUMMARY

In the present work, the luminescence arising from collisions of the gas-phase furan molecules with the low-energy dihydrogen cations has been measured by exploiting collision-induced emission spectroscopy. In particular, the formation of the excited hydrogen atoms and CH radicals has been identified. Our analysis shows that hydrogens may first come from the fragmentation of neutralized $H_2^+$ projectiles. However, we do not exclude the possibility that hydrogen atoms are detached from the closed and/or open furan rings. In contrast, other emitting products result only from furan fragmentation. However, dissociative fragmentation did not appear to be an important process. This is inconsistent with collisions of $H_2^+$ cations with light molecular targets where dissociative fragmentation of the target was the dominant process and charge transfer did not play a role.

*Acknowledgements.* This article is based upon work from COST Action CA20129 – Multiscale Irradiation and Chemistry Driven Processes and Related Technologies, supported by COST (European Cooperation in Science and Technology). The experiments were carried out at the University of Gdansk using a spectrometer for collision-induced emission spectroscopy. Therefore, the author thanks professors A. Kowalski (Univ. of Gdansk) and B. Pranszke (Gdynia Maritime Univ.) for enabling the present measurements.

REFERENCES

1. M. Larsson et al., Rep. Prog. Phys. **75**, 066901 (2012).
2. R.I. Kaiser et al., J. Phys. Chem. A **125**, 3826 (2021).
3. I. Utke et al., J. Vac. Sci. Technol. B **26**, 1197 (2008).
4. U. Amaldi et al., Rep. Prog. Phys. **68**, 1861 (2005).
5. J. Thariat et al., Int. J. Mol. Sci. **21**, 133 (2019).
6. M. A. Huels et al., J. Am. Chem. Soc. **125**, 4467 (2003)
7. C.O. Kappe et al., Tetrahedron **53**, 14179–14233 (1997).
8. O.S. Bruinsma, Fuel **67**, 334–340 (1988).
9. P. Sulzer et al. J. Chem. Phys. **125**, 044304 (2006).
10. T. J. Wasowicz, Rom. J. Phys. **67**, 206 (2022).
11. T. J. Wasowicz et al., Int. J. Mol. Sci. **20**, 6022 (2019).
12. T. J. Wasowicz et al., J. Phys.: Conf. Ser. **635** 032055 (2015).
13. T. J. Wasowicz et al., Eur. Phys. J. D **70**, 175 (2016).
14. T.J. Wasowicz et al., J. Phys. Chem. A **119** (4) 581 (2015).
15. T. J. Wasowicz et al., J. Phys. Chem. A **120**, 964 (2016).
16. CSID:7738, http://www.chemspider.com/Chemical-Structure.7738.html (accessed 18:09, May 15, 2024).
17. I. Linert et al., Chem. Phys. Lett. **498**, 27−31 (2010).
18. T. J. Wasowicz et al., Photon. Lett. Pol. **3**, 110 (2011)
19. T. J. Wasowicz, Res. Phys. **18**, 103244 (2020).
20. T.J. Wasowicz, Rom. Rep. Phys. **73**, 203 (2021).
21. T.J. Wasowicz et al., Acta Phys. Pol. A **140**, 228 (2021).
22. T.J. Wasowicz, Int. J. Mol. Sci. **23**, 205 (2022).
23. M. K. Jurkowski et al., Rom. J. Phys. **68**, 203 (2023).
24. M. K. Jurkowski et al., Rom. J. Phys. **68**, 205 (2023).
25. T. J. Wasowicz et al., J. Chem. Phys. **161**, 064304 (2024).
26. T. J. Wasowicz et al., J. Phys. B: At. Mol. Opt. Phys. **47**, 055103 (2014).
27. M. Zubek et al., J. Chem. Phys. **141**, 064301 (2014).
28. T. J. Wasowicz et al., J. Phys. B: At. Mol. Opt. Phys. **50**, 015101 (2017).
29. T. J. Wasowicz et al., Int. J. Mass Spectrom. **449**, 116276 (2020).
30. T. J. Wasowicz et al., Phys. Chem. Chem. Phys. **24**, 19302–19313 (2022).
31. T. J. Wasowicz et al., Phys. Chem. Chem. Phys. **25**, 31655–31666 (2023).
32. T. J. Wasowicz et al., Phys. Rev. A **83**, 033411 (2011).
33. S. G. Lias, *Ionization Energy data* in NIST Chemistry WebBook, NIST Standard Reference Database Number 69, Eds. P.J. Linstrom and W.G. Mallard, National Institute of Standards and Technology, Gaithersburg MD, 20899, https://doi.org/10.18434/T4D303, (retrieved August 7, 2024).
34. H.E. Bethe, E.E. Salpeter, *Quantum Mechanics of One- and Two-Electron Atoms*, Plenum, New York 1977.
35. T.J. Wasowicz et al., J. Phys. B At. Mol. Opt. Phys. **45**, 205103 (2012).
36. L. Windholz et al., Phys. Scr. **78**, 065303 (2008).
37. L. Windholz et al., J. Opt. Soc. Am. B **29**, 934–943 (2012).
38. R. Drozdowski et al., Chem. Phys. **483-484**, 78–83 (2017).